Available online at www.sciencedirect.com

ScienceDirect

journal homepage: www.elsevier.com/locate/he

Insights into the hydrogen dissociation mechanism on lithium edge-decorated carbon rings and graphene nanoribbon

Alejandro Vásquez-Espinal [a], Ricardo Pino-Rios [a], Patricio Fuentealba [b,c], Walter Orellana [d,**], William Tiznado [e,*]

[a] Doctorado en Fisicoquímica Molecular, Facultad de Ciencias Exactas, Universidad Andres Bello, República 275, Santiago, Chile

[b] Departamento de Física, Universidad de Chile, Las Palmeras 3425, Santiago, Chile

[c] Centro para el Desarrollo de la Nanociencia y Nanotecnologia, CEDENNA, A. Ecuador 3493, Santiago, Chile

[d] Departamento de Ciencias Físicas, Facultad de Ciencias Exactas, Universidad Andres Bello, República 220, Santiago, Chile

[e] Departamento de Ciencias Químicas, Facultad de Ciencias Exactas, Universidad Andres Bello, República 275, Santiago, Chile

ARTICLE INFO

Article history:
Received 25 November 2015
Received in revised form
24 January 2016
Accepted 3 February 2016
Available online 12 March 2016

Keywords:
Hydrogen dissociation
Ab initio calculations
Carbon-lithium systems

ABSTRACT

The purpose of this study is to show that H_2 is easily dissociated on lithium edge decorated carbon systems to form strong C–H and Li–H bonds. This mechanism has not been considered in previous studies where these kinds of systems have been proposed as good candidates to serve as hydrogen storage materials. The reactivity of molecular hydrogen (H_2) on three representative lithium edge-decorated carbon systems (on the clusters $C_5Li_7^+$ (1) and C_6Li_6 (2), and on lithium edge-decorated zig-zag graphene nanoribbon (GNR-Li) (3)) have been studied using ab initio calculations based on the density functional theory with dispersion-corrected van der Waals exchange correlation functional. Our calculations show, on the one hand, that heterolytic hydrogen dissociation can precede with relatively low reaction barriers (0.60, 0.45 and 0.56 eV for systems 1, 2 and 3, respectively) along the minimum energy path and, on the other hand, that chemisorption energies are highly stabilizing (in the range of 1.15–1.54 eV). It is important to note that the highest activation barrier is found for the unique system, characterized as global minimum, on its corresponding potential energy surface (PES), which is system 1. These findings suggest that reversibility of the hydrogen absorption/desorption reactions, required in promising hydrogen storage materials, does not apply in these systems.

* Corresponding author.
** Corresponding author.
E-mail addresses: worellana@unab.cl (W. Orellana), wtiznado@unab.cl (W. Tiznado).

http://dx.doi.org/10.1016/j.ijhydene.2016.02.018

Introduction

The development of reliable and environmentally friendly approaches for energy conversion and storage is one of the key challenges that our society is facing nowadays [1–5]. Fuel cell devices, in which electrical energy is generated by the conversion of chemical energy via redox reactions at the anode and cathode, have now become a major research area [6–10]. The chemical energy density of hydrogen is 142 MJ/kg, which is more than three times the one of gasoline and the by-product of its combustion is water. Thus, hydrogen is one of the most interesting "green" fuels. In this context, graphene and derived compounds, have been proposed as reliable materials that can help to address the two main issues related to the use of hydrogen as fuel: (i) production and (ii) storage/transportation [11–18].

Even though both issues are important, we will now turn our attention to the latter. Many theoretical investigations suggest that the adsorption capacity of hydrogen on graphene is increased by suitable metal doping modifications, thus making two kinds of molecular interactions possible. The first one is based on the polarization of H_2 by the electric field established by alkali, or earth alkali metals, leading to H_2 binding energies of approximately 0.2 eV [19–23]. The second one is based on the so-called Kubas interactions [24], where the transition metal orbitals are combined with the hydrogen orbitals to achieve binding energies between 0.2 and 0.6 eV. These stabilizing interactions make these materials potentially useful for hydrogen storage [25–29].

Motivated by this increasing need for suitable hydrogen storage materials, other researchers have focused on testing other carbon-based materials. For instance, Sun and co-workers proposed, *in silico*, the cluster $Li_{12}C_{60}$ (where each Li was individually placed in order to cap each of the twelve pentagons of the fullerene) as a potential hydrogen storage system [19]. The authors suggested that, due to the difference in electronegativity between Li and C, the Li atoms have a positive partial charge, favoring an ion-induced dipole electrostatic interaction with the H_2 molecule; which, in turn, induces the H_2 adsorption on this system.

More recently, two lithium edge decorated carbon aromatic clusters have been proposed as promising systems for hydrogen storage [30–33]: the hexalithium benzene (C_6Li_6) and the $C_5Li_7^+$ cluster [34]. It is important to note that the star-shape is the global minimum energy structure for $C_5Li_7^+$, for C_6Li_6 it is only a local minimum on the corresponding potential energy surface [35].

Quantum chemical calculations predicted that the first one can trap between 6 and 12H_2 molecules (involving a non-dissociative H_2 interaction) with a good gravimetric weight percentage of adsorbed hydrogen (9.6 wt%) [30,32]. Whereas in the second one, each Li center can bind up to three H_2 molecules, which leads to a noticeable gravimetric weight percentage (28.0 wt%) [31]. However, this exceptional hydrogen storage capability is supported only on the non-dissociative H_2 adsorption on the cluster surface. Moreover, different to what happens in lithium doped graphene sheets, fullerenes and nanotubes (where lithium is bonded by electrostatic interactions involving lithium and the delocalized π-cloud of the systems) [19,36], in lithium edge decorated carbon systems, it is expected that electrostatic interaction, between lithium and carbon, mainly involves the σ-cloud of the systems. This has important implications on the reactivity of H_2 on this class of materials.

In order to gain a better understanding of the H_2 interaction with any chemical system, it is mandatory to evaluate the viability of the H_2 dissociative adsorption. If the H_2 dissociation were an energetically favored process, it would have two key implications: on the one hand, the chemisorption would change drastically the H_2 release energies; and on the other hand, the cleavage and formation of new chemical bonds could transform the material irreversibly.

In this work we present a computational study to explore the energetic viability and the mechanism involved in a dissociative interaction of H_2 with three representative lithium edge-decorated carbon systems. The first two are the clusters $C_5Li_7^+$ (1) and C_6Li_6 (2) mentioned above. Whereas, system 3 consists of a lithium-decorated zig-zag graphene nanoribbon (GNR-Li), with periodicity along the zig-zag direction, as depicted in Scheme 1.

Computational methods

As a first approximation on the H_2 interaction with the C–Li clusters (systems 1 and 2), collisions between one H_2 molecule and these systems were performed. They were simulated using Born–Oppenheimer molecular dynamics (BO–MD) [37], with a time step of 1 fs and the total time of the dynamics was 5 ps. The temperature was fixed at 273 K and, in order to keep the total nuclear energy fixed, the velocities were rescaled at each step. These calculations were performed at the ωB97X-D

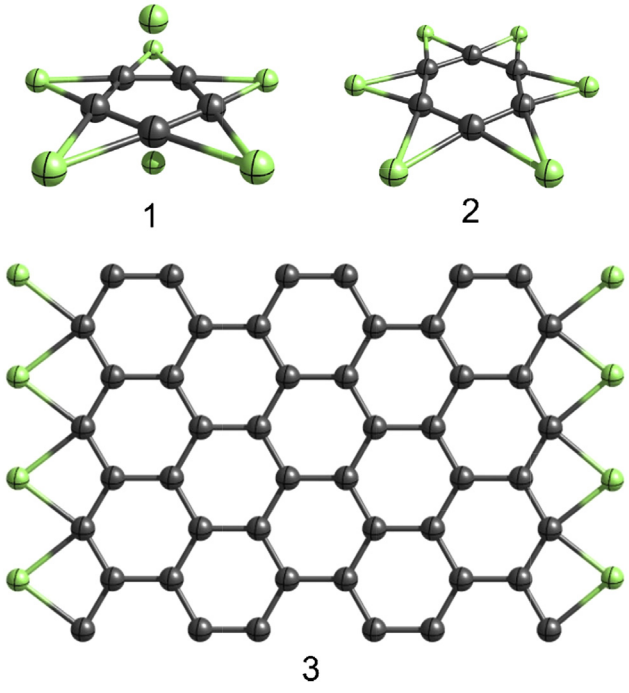

Scheme 1 – Equilibrium geometries of the three systems under study: $C_5Li_7^+$ (1), C_6Li_6 (2) and GNR-Li (3).

[38]/6-31G(d) level using the Gaussian09 program [39]. Since this program only includes the velocity rescaling type of thermostat in the ADMP (atom centered density matrix propagation) [40] dynamics, we ran the ADMP dynamics with the FULLSCF option, which is equivalent to a BO–MD.

The energetic, structural and electronic changes in H_2 dissociation process on the 1–3 species were analyzed by assessing the minimum energy path, identifying a first order saddle point (transition state (TS)) that connects the corresponding reagents and products. This was performed using two theoretical approximations with the aim of comparing and ensuring the validity of our predictions.

Firstly, the maximum energy structures obtained in the BO–MD calculations were optimized searching for a first order saddle point (characterized by one imaginary frequency) using the Berny algorithm [41]. Then, it was verified that these TSs connect the corresponding reagents and products of the hydrogen dissociation reaction on systems 1 and 2 by means of the intrinsic reaction coordinate (IRC) calculations [39]. Geometry optimizations, frequency analysis and IRC calculations were done at the ωB97X-D/6-311G(d,p) level with the Gaussian09 program.

Secondly, the nudged elastic band (NEB) method was used [42,43] to search the minimum energy path of the hydrogen dissociation reaction on systems 1 to 3, identifying the corresponding TSs. This method works by optimizing a number of intermediate structures along the reaction path. In our approach, the H_2 dissociation paths were estimated using ten intermediate structures. For the initial configuration, we considered the optimized geometry of H_2 at 5 Å from a C atom of each of the analyzed systems. Whereas for the final configuration, one of the adsorbed hydrogen was bonded to one C atom and, the second one was being a part of a lithium hydride cluster. NEB calculations were performed using spin-polarized density functional theory (DFT) calculations, implemented in the Quantum Espresso ab-initio package [44]. For the exchange and correlation term, we used the dispersion-corrected van der Waals density functional approach [45]. Kohn-Sham eigenfuctions were expanded on a plane-wave basis set, where the interaction between valence electrons and ion cores were described by ultra-soft pseudopotentials. Converged results were achieved by using cutoff energies of 30 Ry on the plane wave and of 180 Ry on the electronic density.

To build the unit cell of the GNR-Li (system 3), we used the unit cell of a zig-zag graphene nanoribbon of 11.5 Å width and decorated it at both edges with Li atoms, following the same configuration of the carbon clusters, as shown in Scheme 1. The GNR-Li system was described within a cubic supercell with a volume of a_0 x 30 × 15 Å^3, where a_0 = 9.866 Å is the periodicity along the zigzag direction. Whereas, for the C_6Li_6 and $C_5Li_7^+$ clusters, we used a supercell with a volume of 20 × 20 × 15 Å^3. For the Brillouin zone sampling we considered the Γ point for the three structures. The systems were fully relaxed until the residual force on each atomic component was less than 0.025 eV/Å.

In order to gain further insight into the chemical bonding evolution along the reaction coordinate, the adaptive natural density partitioning (AdNDP) [46] method was used. The AdNDP method analyses the first order reduced density matrix in order to represent the electronic structure of a given system in terms of n-center-two-electron (nc–2e) elements, where n can take values from 1 to 2 which accounts for localized bonding elements (1c–2e or 2c–2e, i.e. lone pairs and two-center two-electron σ or π bonds) up to the total number of atoms (delocalized bonding elements).

The full-density matrix in the basis of the natural atomic orbitals, as well as the transformation between the atomic orbital and the natural atomic orbital basis sets, were generated at the ωB97X-D/6-311G(d,p) level using the NBO 3.1 code [47] incorporated into Gaussian09. The AdNDP analysis was performed using the Multiwfn program [48].

Results and discussion

At first, we were interested in knowing what happens when one hydrogen molecule collides with the systems 1–2. To model this process, we used BO–MD calculations to simulate the impact of an H_2 molecule (projectile) on the clusters 1 and 2 (targets). Due to the small size of these clusters, it was possible to explore different impact trajectories using an adequate level at a relatively short period of time. The relative orientations considered in the simulations are illustrated in Scheme 2. Initially, the H_2 center of mass was placed at 9 Å apart from one of the carbons of the clusters. To avoid a huge number of configurations, we restricted the relative orientations only to the ones shown in the scheme, changing both the distance b (from 0 to 1 Å) and the angle, a (from 0° to 90°). In

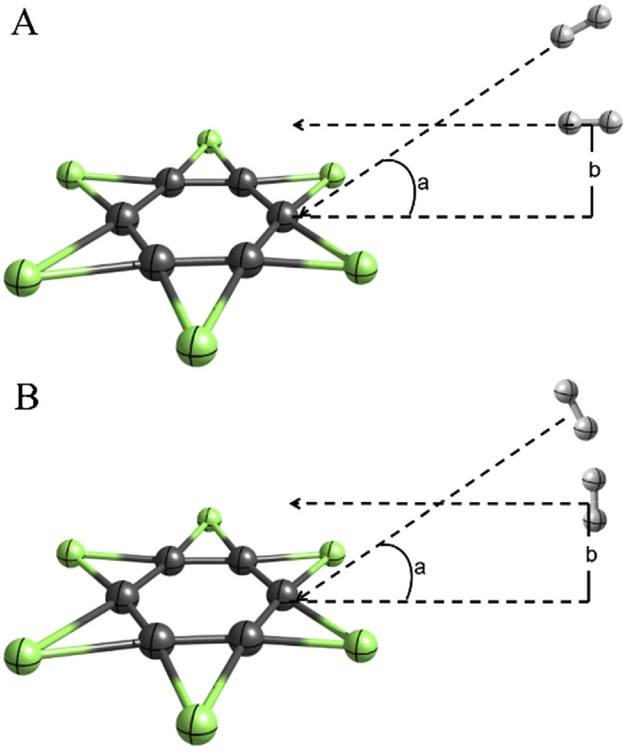

Scheme 2 – Collision setup used in the BO–MD, the parameters considered were b = 0.00 Å, 0.25 Å, 0.50 Å, 0.75 Å, 1.00 Å and a = 0.0°, 30.0°, 45.0°, 90.0°.

addition, the initial velocities were restricted to be longitudinal, transverse or angular to the H_2 (see scheme).

At the beginning of the collision, the clusters were at rest. Initial velocities of H_2 were assigned according to the temperature (see computational details). In the case of the interaction between H_2 and system 1, the BO–MD showed that hydrogen dissociation takes place at both, an impact parameter of 0.50 Å or lower and, at angles equal to 0° and 30° according to collision setup A (see Scheme 2). A similar trend was observed for the interaction between H_2 and system 2. However, in the second case, the hydrogen molecule dissociates even at an impact parameter of 0.75 Å (or 0°, 30° and 45°). Over these values, a bouncing back of the hydrogen molecule is observed. In the case of collision setup B (see Scheme 2) the bouncing back of the hydrogen molecule was observed for all of the parameters considered. The potential energy profiles along the BO–MD simulation for the collision of H_2 against systems 1 and 2 (with an impact parameter of 0 Å and a collision angle of 0°) are shown in Figs. 1 and 2, respectively. The remaining potential energy profiles (for the other collision parameters considered) are available in the supporting information (Fig. 1-SI to 4-SI).

The BO–MD trajectories allowed us to identify one maximum energy structure (II) and three minimum energy structures (I, III, IV) as shown in Figs. 1 and 2. The dynamics showed that in structure II, the H_2 is bonded, by one of the hydrogen atoms, to one of the carbon atoms. Then, the dissociation proceeds by migration of the other hydrogen towards one neighboring Li (this process occurs during structure II to structure III transformation). Finally, the local minimum III is relaxed to a low-energy isomer IV, where it is clearly observed that H_2 dissociates to form a –CH group and a LiH hydride. The trajectory dependence and the formation of a C–H bond observed on the dissociative process, suggests that reaction proceeds through the σ-electrons on the C–Li systems (large figures and Cartesian coordinates of the structures I–IV are depicted in Tables 1-SI and 2-SI in the supporting information).

Energetically and structurally, the H_2 dissociative process, according to the BO–MD analysis is similar on both aromatic clusters, which leads us to ask the following questions: are the

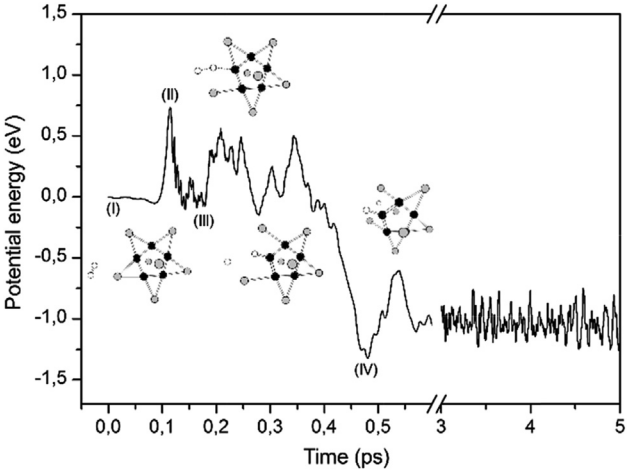

Fig. 1 – Collision between H_2 and $C_5Li_7^+$ simulated at 273 K. Impact parameter b = 0 Å, collision angle 0°.

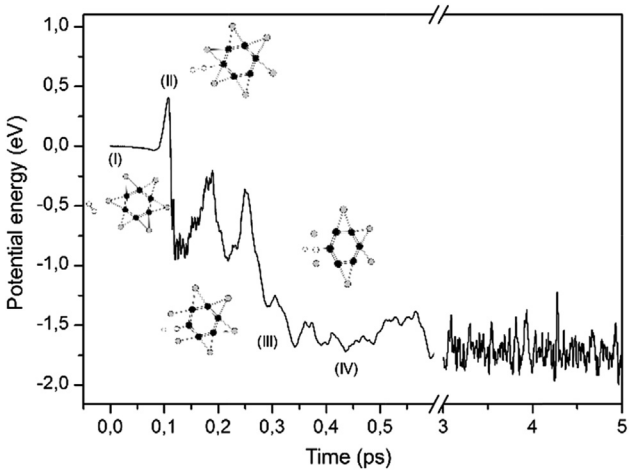

Fig. 2 – Collision between H_2 and C_6Li_6 simulated at 273 K. Impact parameter b = 0 Å, collision angle 0°.

$C_5Li_7^+$ and C_6Li_6 systems the only Li edge-decorated carbon rings that easily dissociate H_2? Or is it a general pattern for this kind of molecules? For example, can H_2 be easily dissociated on a GNR-Li (system 3)?

In an attempt to answer these questions, we calculated the activation energy (AE) barriers for H_2 dissociation on the C–Li analyzed systems. In order to do this, we identified the TSs using, as a starting point, the maximum energy structures of the BO–MD (see computational details). The AE barriers obtained from this approximation are of 0.66 and 0.38 eV for systems 1 and 2, respectively. These barriers are similar to those observed in the BO–MDs. So, the picture of the reaction process obtained from BO-MD simulations, are confirmed by transition state search (see IRCs in Fig. 5-SI in the supporting information). Finally, in order to estimate the AE barrier of the H_2 dissociation on the three analyzed systems, the minimum energy path was calculated using the NEB method (see computational details). The reaction profiles for H_2 dissociation are shown in Fig. 3. The activation energy barriers were

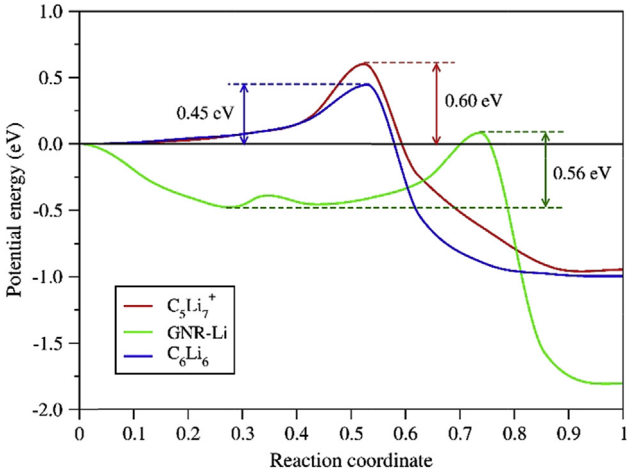

Fig. 3 – Minimum energy paths for H_2 dissociation on the $C_5Li_7^+$ and C_6Li_6 clusters, and on the Li-decorated zig-zag graphene nanoribbon (GNR-Li).

found to be of 0.60, 0.45 and 0.56 eV, for systems 1, 2 and 3, respectively. It is important to note that the highest activation barrier is found for the unique system, characterized as global minimum, on its corresponding PES, which is system 1. The results for system 1 and 2 were in good agreement with those obtained with the BO–MD and IRC formalism, within variations of about 0.07 eV, which supports the quality of our NEB calculations, thus allowing a good estimation for the H_2 dissociation energy in an extended system like GNR-Li.

We also evaluated the energetic changes involved in the following gas-phase reactions:

$$C_5Li_7^+(D_{5h}) + 5H_2\ (D_{\infty h}) \rightarrow Li_7C_5H_{10}^+\ (C_1) \quad (1)$$

$$C_6Li_6(D_{6h}) + 6H_2\ (D_{\infty h}) \rightarrow Li_6C_6H_{12}\ (C_1) \quad (2)$$

Surprisingly, we found that these gas-phase reactions are highly exothermic ($\Delta E = -6.2$ eV and $\Delta E = -9.2$ eV at the ωB97X-D/6-311G(d,p) level for reaction (1) and (2), respectively). The structures of the reaction products in 1 and 2, clearly allows to identify the cyclopentadienyl lithium and the benzene into the complexes $Li_7C_5H_{10}^+$ and $Li_6C_6H_{12}$, respectively (see structures and coordinates in Fig. 6-SI and 7-SI). These results show that hydrogenation of the clusters 1 and 2, is an energetically favored process that regenerates the classic aromatic hydrocarbons, from which the initial clusters are their inorganic analogues.

Chemical bonding analysis

An inspection of the canonical molecular orbitals (CMOs) of the TSs, as well as of the reactants for the H_2 dissociation reaction on 1 and 2, showed that the highest occupied molecular orbital (HOMO) of 1 and 2, combines with the lowest unoccupied molecular orbital (LUMO) of H_2 to form an early C–H bond in the TS. Therefore, it suggests that the dissociation of H_2 is promoted by an initial bonding interaction between the HOMO of 1 and 2 (which is mainly localized on the carbon like a lone pair) and the empty H_2 σ^*-orbital (see Fig. 8-SI and 9-SI in the supporting information).

In order to gain more insight on how chemical bonding changes during the reaction of H_2 with systems 1 and 2, the AdNDP method was applied to the four selected structures along the reaction path (I–IV). The AdNDP results for systems 1 and 2 are shown in Figs. 4 and 5, respectively. In the figures, the π-electronic structure is not included because it remains constant along the reaction path (see the complete AdNDP pictures in Figs. 10-SI to 19-SI). The chemical bonding evolution allows us to interpret that the heterolytic dissociation of H_2, to form a –CH group and a LiH hydride, is promoted by an initial bonding interaction between one 3c–2e Li–C–Li σ- and

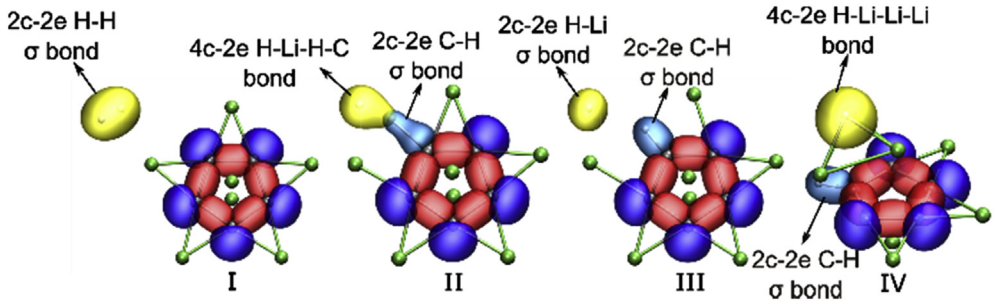

Fig. 4 – Chemical bonding pattern revealed for the different local minima and TS of the $C_5Li_7^+$-H_2 system using the AdNDP method. There are reported only the σ-bonds and lone pairs (LP) for clarity.

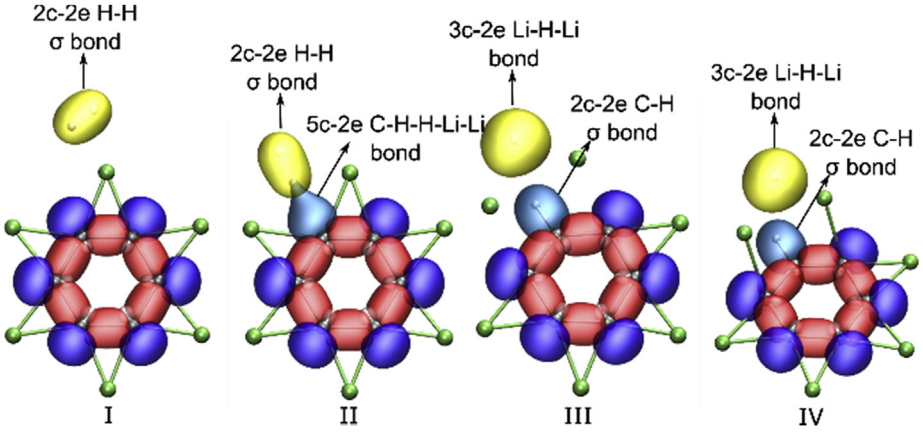

Fig. 5 – Chemical bonding pattern revealed for the different local minima and TS of the C_6Li_6–H_2 system using the AdNDP method. There are reported only the σ-bonds and lone pairs (LP) for clarity.

one empty H_2 σ^*-orbital (at TS, II) in agreement with the preliminary CMO analysis.

Conclusions

The reactivity of molecular hydrogen (H_2) on three representative lithium edge-decorated carbon systems (on the clusters $C_5Li_7^+$ (1) and C_6Li_6 (2), and on lithium edge-decorated zig-zag graphene nanoribbon (GNR-Li) (3)) have been studied using ab initio calculations based on the density functional theory with dispersion-corrected van der Waals exchange correlation functional. The calculations showed that hydrogen dissociation on these systems is kinetic and energetically favored. These conclusions are supported by the analysis of the minimum energy reaction path, which shows relatively low reaction barriers (in the range of 0.38–0.66 eV) and highly stabilizing chemisorption energies (in the range of 1.15–1.54 eV). It is important to note that the highest activation barrier is found for the unique system, characterized as global minimum, on its corresponding PES, which is system 1. Additionally, at 273 K, the Born–Oppenheimer molecular dynamics (BO–MD) simulations showed that reactions proceed effectively as long as they follow trajectories closer to the molecular plane. Finally, the chemical bonding analysis shows that the heterolytic dissociation of H_2, to form a –CH group and a LiH hydride, is promoted by an initial bonding interaction between one 3c-2e Li–C–Li σ- and one empty H_2 σ^*-orbital. These results suggest that reversibility of the hydrogen absorption/desorption reactions (required in promising hydrogen storage materials) does not apply in these systems.

Acknowledgments

The authors are grateful for the financial support of the grants: Fondecyt 1140358 and 1130202, CONICYT-PIA under the Grant Anillo ACT-1107, CONICYT-PCHA/Doctorado Nacional/2013-633130043, Center for the Development of Nanoscience and Nanotechnology CEDENNA FB0807, and Universidad Andres Bello (DI-619-14/I and DI-781-15/I).

Appendix A. Supplementary data

Supplementary data related to this article can be found at http://dx.doi.org/10.1016/j.ijhydene.2016.02.018.

REFERENCES

[1] Schlapbach L, Zuttel A. Hydrogen-storage materials for mobile applications. Nature 2001;414:353–8.
[2] Eberle U, Felderhoff M, Schüth F. Chemical and physical solutions for hydrogen storage. Angew Chem Int Ed 2009;48:6608–30.
[3] Jain IP. Hydrogen the fuel for 21st century. Int J Hydrogen Energy 2009;34:7368–78.
[4] Liu C, Li F, Ma L-P, Cheng H-M. Advanced materials for energy storage. Adv Mater 2010;22:E28–62.
[5] Jena P. Materials for hydrogen storage: past, present, and future. J Phys Chem Lett 2011;2:206–11.
[6] Hickner MA, Ghassemi H, Kim YS, Einsla BR, McGrath JE. Alternative polymer systems for Proton Exchange Membranes (PEMs). Chem Rev. 2004;104:4587–612.
[7] Borup R, Meyers J, Pivovar B, Kim YS, Mukundan R, Garland N, et al. Scientific aspects of polymer electrolyte fuel cell durability and degradation. Chem Rev. 2007;107:3904–51.
[8] Diat O, Gebel G. Fuel cells: proton channels. Nat Mater 2008;7:13–4.
[9] Wagner FT, Lakshmanan B, Mathias MF. Electrochemistry and the future of the automobile. J Phys Chem Lett 2010;1:2204–19.
[10] Dodds PE, Staffell I, Hawkes AD, Li F, Grünewald P, McDowall W, et al. Hydrogen and fuel cell technologies for heating: a review. Int J Hydrogen Energy 2015;40:2065–83.
[11] Bonaccorso F, Colombo L, Yu G, Stoller M, Tozzini V, Ferrari AC, et al. Graphene, related two-dimensional crystals, and hybrid systems for energy conversion and storage. Science 2015:347.
[12] Yürüm Y, Taralp A, Veziroglu TN. Storage of hydrogen in nanostructured carbon materials. Int J Hydrogen Energy 2009;34:3784–98.
[13] Yadav S, Tam J, Singh CV. A first principles study of hydrogen storage on lithium decorated two dimensional carbon allotropes. Int J Hydrogen Energy 2015;40:6128–36.
[14] Rangel E, Ramírez-Arellano JM, Carrillo I, Magana LF. Hydrogen adsorption around lithium atoms anchored on graphene vacancies. Int J Hydrogen Energy 2011;36:13657–62.
[15] Kim D, Lee S, Hwang Y, Yun K-H, Chung Y-C. Hydrogen storage in Li dispersed graphene with Stone–Wales defects: a first-principles study. Int J Hydrogen Energy 2014;39:13189–94.
[16] Li P, Deng SH, Zhang L, Liu GH, Yu JY. Hydrogen storage in lithium-decorated benzene complexes. Int J Hydrogen Energy 2012;37:17153–7.
[17] Seenithurai S, Pandyan RK, Kumar SV, Saranya C, Mahendran M. Li-decorated double vacancy graphene for hydrogen storage application: a first principles study. Int J Hydrogen Energy 2014;39:11016–26.
[18] Xu B, Lei XL, Liu G, Wu MS, Ouyang CY. Li-decorated graphyne as high-capacity hydrogen storage media: first-principles plane wave calculations. Int J Hydrogen Energy 2014;39:17104–11.
[19] Sun Q, Jena P, Wang Q, Marquez M. First-principles study of hydrogen storage on $Li_{12}C_{60}$. J Am Chem Soc. 2006;128:9741–5.
[20] Chandrakumar KRS, Ghosh SK. Alkali-metal-induced enhancement of hydrogen adsorption in C_{60} fullerene: an ab initio study. Nano Lett. 2008;8:13–9.
[21] Yoon M, Yang S, Hicke C, Wang E, Geohegan D, Zhang Z. Calcium as the superior coating metal in functionalization of carbon fullerenes for high-capacity hydrogen storage. Phys Rev Lett. 2008;100:206806.
[22] Wang Q, Sun Q, Jena P, Kawazoe Y. Theoretical study of hydrogen storage in Ca-coated fullerenes. J Chem Theory Comput 2009;5:374–9.
[23] Yoon M, Yang S, Wang E, Zhang Z. Charged fullerenes as high-capacity hydrogen storage media. Nano Lett. 2007;7:2578–83.
[24] Kubas GJ. Metal-dihydrogen and σ-bond coordination: the consummate extension of the Dewar-Chatt-Duncanson model for metal-olefin π bonding. J Organomet Chem. 2001;635:37–68.

[25] Zhao Y, Kim Y-H, Dillon AC, Heben MJ, Zhang SB. Hydrogen storage in novel organometallic buckyballs. Phys Rev Lett. 2005;94:155504.
[26] Yildirim T, Ciraci S. Titanium-decorated carbon nanotubes as a potential high-capacity hydrogen storage medium. Phys Rev Lett. 2005;94:175501.
[27] Park N, Hong S, Kim G, Jhi S-H. Computational study of hydrogen storage characteristics of covalent-bonded graphenes. J Am Chem Soc. 2007;129:8999–9003.
[28] Durgun E, Ciraci S, Yildirim T. Functionalization of carbon-based nanostructures with light transition-metal atoms for hydrogen storage. Phys Rev B 2008;77:085405.
[29] Spyrou K, Gournis D, Rudolf P. hydrogen storage in graphene-based materials: efforts towards enhanced hydrogen absorption. ECS J Solid State Sci Technol 2013;2:M3160–9.
[30] Giri S, Lund F, Núñez AS, Toro-Labbé A. Can starlike C_6Li_6 be treated as a potential H_2 storage material? J Phys Chem C 2013;117:5544–51.
[31] Pan S, Merino G, Chattaraj PK. The hydrogen trapping potential of some Li-doped star-like clusters and super-alkali systems. Phys Chem Chem Phys 2012;14:10345–50.
[32] Giri S, Bandaru S, Chakraborty A, Chattaraj PK. Role of aromaticity and charge of a system in its hydrogen trapping potential and vice versa. Phys Chem Chem Phys 2011;13:20602–14.
[33] Tang C, Gao F, Zhang Z, Kang J, Zou J, Xu Y, et al. The properties of hydrogenated derivatives of the alkali atom coated clusters C_6M_6 (M = Li, Na): a density functional study. Comput Theor Chem 2015;1071:46–52.
[34] Perez-Peralta N, Contreras M, Tiznado W, Stewart J, Donald KJ, Merino G. Stabilizing carbon-lithium stars. Phys Chem Chem Phys 2011;13:12975–80.
[35] Moreno D, Martínez-Guajardo G, Díaz-Celaya A, Mercero JM, de Coss R, Perez-Peralta N, et al. Re-examination of the C_6Li_6 structure: To Be, or not to be symmetric. Chem Eur J 2013;19:12668–72.
[36] Liu W, Zhao YH, Li Y, Jiang Q, Lavernia EJ. Enhanced hydrogen storage on Li-dispersed carbon nanotubes. J Phys Chem C 2009;113:2028–33.
[37] Millam JM, Bakken Vr, Chen W, Hase WL, Schlegel HB. Ab initio classical trajectories on the Born–Oppenheimer surface: Hessian-based integrators using fifth-order polynomial and rational function fits. J Chem Phys 1999;111:3800–5.
[38] Chai J-D, Head-Gordon M. Long-range corrected hybrid density functionals with damped atom-atom dispersion corrections. Phys Chem Chem Phys 2008;10:6615–20.
[39] Frisch MJ, Trucks GW, Schlegel HB, Scuseria GE, Robb MA, Cheeseman JR, et al. Gaussian 09, Revis. C.01. Wallingford CT: Gaussian, Inc.; 2010.
[40] Schlegel HB, Millam JM, Iyengar SS, Voth GA, Daniels AD, Scuseria GE, et al. Ab initio molecular dynamics: propagating the density matrix with Gaussian orbitals. J Chem Phys 2001;114:9758–63.
[41] Li X, Frisch MJ. Energy-represented direct inversion in the iterative subspace within a hybrid geometry optimization method. J Chem Theory Comput 2006;2:835–9.
[42] Mills G, Jónsson H. Quantum and thermal effects in H_2 dissociative adsorption: evaluation of free energy barriers in multidimensional quantum systems. Phys Rev Lett. 1994;72:1124–7.
[43] Henkelman G, Jónsson H. Improved tangent estimate in the nudged elastic band method for finding minimum energy paths and saddle points. J Chem Phys 2000;113:9978–85.
[44] Gianozzi P, Baroni S, Bonini N, Calandra M, Car R, Cavazzoni C, et al. Quantum ESPRESSO: a modular and open-source software project for quantum simulations of materials. J Phys: Condens Matter 2009;21:395502.
[45] Dion M, Rydberg H, Schröder E, Langreth DC, Lundqvist BI. Van der Waals density functional for general geometries. Phys Rev Lett. 2004;92:246401.
[46] Zubarev DY, Boldyrev AI. Developing paradigms of chemical bonding: adaptive natural density partitioning. Phys Chem Chem Phys 2008;10:5207–17.
[47] Glendening E, Reed A, Carpenter J, Weinhold F. NBO, version 3.1. 1998.
[48] Lu T, Chen F. Multiwfn: a multifunctional wavefunction analyzer. J Comput Chem. 2012;33:580–92.